



## Article

# Comparison of Lake Ice Extraction Methods Based on MODIS Images

Hongfang Zhang <sup>1,2</sup>, Xiaojun Yao <sup>1,2,\*</sup> , Qixin Wei <sup>1,2</sup>, Hongyu Duan <sup>1,2</sup> and Yuan Zhang <sup>1,2</sup><sup>1</sup> College of Geography and Environmental Science, Northwest Normal University, Lanzhou 730070, China<sup>2</sup> Key Laboratory of Resource Environment and Sustainable Development of Oasis, Lanzhou 730070, China

\* Correspondence: xj\_yao@nwnu.edu.cn; Tel.: +86-131-0930-9241

**Abstract:** As an important part of the cryosphere, lake ice is a sensitive indicator of climate change. Remote sensing technology can quickly and accurately monitor the process of its formation and decay, among which Moderate Resolution Imaging Spectroradiometer (MODIS) images are the most widely used data in the remote sensing monitoring of lake ice. The reasonable selection of monitoring methods is of great significance to grasp the dynamic process and response to climate change of lake ice. In this study, five commonly used remote sensing monitoring methods of lake ice based on MODIS MOD09GA data, including the single band threshold method (SBT), reflectance difference threshold method (RDT), normalized difference snow index method (NDSI), modified normalized difference snow index method (MNDSI) and lake ice index method (LII), were selected to compare their accuracies in extracting lake ice extent by combining them with four evaluation metrics of accuracy, precision, recall and mean intersection over union (MIoU). In addition, the ability of the high-precision LII method for extracting long time series lake ice phenology and its applicability to multiple types of lakes were verified. The results showed that compared with the NDSI method, the other four methods more easily distinguished between lake ice and lake water by setting thresholds. The SBT method and the RDT method had better extraction effects in the freezing process and the melting process, respectively. Compared with the NDSI and MNDSI methods, the LII method showed a significant improvement in lake ice extraction over the entire freeze–thaw cycle, with the smallest mean monitoring error of 1.53% for the percentage of lake ice area in different periods. Meanwhile, the LII method can be used to determine long term lake ice phenology dates and had good performance in extracting lake ice for different types of lakes on the Qinghai–Tibet Plateau with the optimal threshold interval of 0.05–0.07, which can be used for lake ice monitoring and long-term phenological studies in this region.

**Keywords:** lake ice; phenology; MODIS; Qinghai Lake; Qinghai–Tibet Plateau

**Citation:** Zhang, H.; Yao, X.; Wei, Q.; Duan, H.; Zhang, Y. Comparison of Lake Ice Extraction Methods Based on MODIS Images. *Remote Sens.* **2022**, *14*, 4740. <https://doi.org/10.3390/rs14194740>

Academic Editors: Anshuman Bhardwaj, Lydia Sam and Saeideh Gharehchahi

Received: 18 July 2022

Accepted: 19 September 2022

Published: 22 September 2022

**Publisher's Note:** MDPI stays neutral with regard to jurisdictional claims in published maps and institutional affiliations.



**Copyright:** © 2022 by the authors. Licensee MDPI, Basel, Switzerland. This article is an open access article distributed under the terms and conditions of the Creative Commons Attribution (CC BY) license (<https://creativecommons.org/licenses/by/4.0/>).

## 1. Introduction

The “AR6 Climate Change 2021: The Physical Science Basis” released by the United Nations Intergovernmental Panel on Climate Change (IPCC) points out that the Earth’s surface has been warming faster than previously expected. The global average surface temperature has risen by about 1 °C since 1850–1900 and is expected to increase by 1.5 °C in the next few decades [1]. Lakes are important components of the Earth system, covering about 3.7% of the global non-glaciated land surface [2], and are the key link between the atmosphere, hydrosphere and cryosphere [3,4]. Lake ice forms during the cold season and is more sensitive to slight changes in climatic conditions than factors such as lake morphology, probably better than weather records themselves [5]. Therefore, lake ice was identified as one of the Essential Climate Variables (ECVS) by the Global Climate Observing System (GCOS) of the World Meteorological Organization (WMO) [6]. There are significant correlations between lake ice phenology events (the date and duration of lake freezing and thawing) and air temperature, and thus these lake phenological records are seen as

an effective indicator of regional climate change [7]. The Qinghai–Tibet Plateau (QTP) possesses the largest cryosphere system in the middle and low latitudes of the Earth and is one of the focus areas of Earth science research. It has been warming more than twice as fast as the globe in recent decades, which has had a profound impact on the region’s cryosphere elements such as lake ice [3]. Many lakes are widely distributed on the QTP, and their phase changes in the freeze–thaw processes alter the thermodynamic interaction between the underlying surface and the atmosphere in this region. Lake ice feeds back to the regional and global climate system and affects regional-scale climate change by changing the mass and energy exchange between water (ice) and the atmosphere [8,9]. Simultaneously, its formation and decay have a direct impact on human production activities and local ecology [10]. Therefore, the research of lake ice on the QTP is important in both theoretical and practical aspects.

As the earliest method to monitor ice phenology, manual observation can be traced back to the 15th century and has obtained the most detailed and temporally extensive climate records [11,12]. However, it requires a lot of manpower and material resources and cannot be applied to remote areas with harsh environments. Meanwhile, further research can face obstacles due to the lack of uniformity in the data obtained. The establishment of lake ice phenology field observation networks has been gradually aborted in many countries and regions [7], but remote sensing has been widely used in lake ice monitoring due to its wide coverage and high monitoring frequency [13]. According to different wavelengths used, the common remote sensing data for lake ice monitoring can be roughly divided into two types: optical remote sensing and microwave remote sensing. Among them, the former (such as NOVA AVHRR, Terra/Aqua MODIS, NPP VIIRS, Landsat TM/ETM+/OLI, Sentinel-2 MSI) extracts lake ice by utilizing the reflection spectrum difference between water and ice [7,14–16], while the latter (such as SMMR, SSM/I, AMSR-E, Radarsat SAR, ENVI-SAT ASAR, Sentinel-1 SAR) obtains lake ice information based on the difference in brightness temperature and backscatter coefficients of lake ice and water [17–19].

Optical images are often used to detect lake ice phenology characteristics and their response to climate change owing to the short revisit cycle and high spatial resolution, but they are greatly affected by cloud cover and illumination conditions. Microwave remote sensing can penetrate clouds and fog and has higher availability in cloudy and high latitude areas [17]. However, the spatial resolution of passive microwave remote sensing images is so low that it is only applicable to lakes with large areas. In contrast to that, active microwave remote sensing has high spatial resolution but low temporal resolution and complex preprocessing steps [20]. It is difficult to find microwave images suitable for detecting lake ice when both temporal and spatial resolution are considered. MODIS data are particularly suitable for capturing long-term changes in seasonal events throughout the year and have become one of the optimum choices for lake ice phenology research because of the short revisit cycle, high spatial resolution (compared with passive microwave remote sensing) and rich spectral information [9,21,22]. Several kinds of data (such as daily MODIS reflectance data, snow products and temperature product) and methods are derived based on MODIS data, which are used to obtain lake ice phenology information or to validate the results from other remote sensing data [13,14,16–18,23–26]. For example, Cai et al. (2018) used MODIS daily snow products to extract the freeze-up start and break-up end dates of 58 lakes on the QTP from 2001 to 2017 and analyzed their spatial variabilities and change rates. The result indicated that the spatial heterogeneity of lake ice phenology is determined by geographical location and climatic conditions, and the duration of ice cover can embody the climate and environmental variation of lakes on the QTP [27]. The selection of reasonable methods and thresholds is key to the accurate extraction of lake ice phenology. However, the problems of multiple methods and multiple threshold selections in previous lake ice remote sensing research works make lake ice products less effective than other cryosphere topics [22,28]. In this study, the effects of five common optical remote sensing monitoring methods based on Terra MODIS MOD09GA data for extracting lake ice phenology were evaluated, and the ability of the lake ice index method

with higher accuracy to monitor long-term lake ice phenology events and its applicability in large regional multi-type lakes were discussed, aiming to provide method support for improving the extraction accuracy of lake ice extent and accurately obtaining lake ice phenology information.

## 2. Study Area

Qinghai Lake ( $36^{\circ}32' \sim 37^{\circ}15'N$ ,  $99^{\circ}36' \sim 100^{\circ}47'E$ ), located in the northeast of the QTP, was formed due to the uplift of surrounding mountains and the blockage of the outflow channel caused by neotectonic movement [25] (Figure 1). As the largest inland brackish water lake in China, it is about 39.8 km and 109 km long in the longitude and latitude directions, respectively, with a total area and perimeter of 4540.46 km<sup>2</sup> and 445 km [29]. Qinghai Lake is situated at the intersection of the western arid zone and eastern monsoon zone in China. It has an alpine and semi-arid continental climate, featuring low annual temperature and large daily temperature difference, with an average annual temperature of  $-1.4 \sim 1.7^{\circ}C$ . The precipitation in this region is low and varies greatly between seasons, mainly concentrated in June to September, with the characteristics of less in the southwest and more in the northeast and increasing from the lake center to the surroundings [30]. Qinghai Lake starts to freeze in December every year, forming a stable ice cover at the end of December or early January in the next year; then, it completely melts in April [25]. The average ice coverage duration, ablation duration, freeze duration and complete freeze duration from 2000 to 2018 were 107 days, 14 days, 86 days and 72 days, respectively [31]. Some studies have stated that the climate in the Qinghai Lake Basin has been getting warmer and more humid in recent years [32]. Meanwhile, the freeze-up date of Qinghai Lake has been delayed while the break-up date has been earlier, and the freezing duration has been significantly shortened [18].

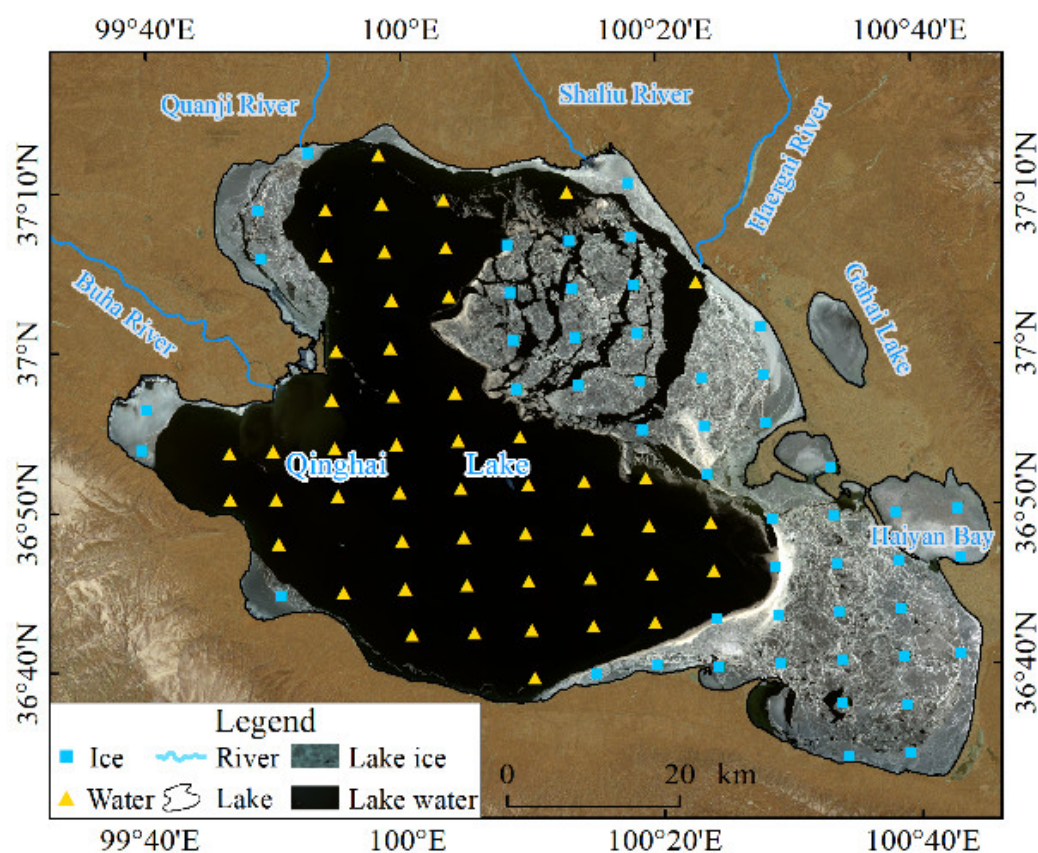


Figure 1. Qinghai Lake (the base map is Landsat OLI image (Bands 5, 4, 3) on 26 March 2017).

### 3. Data and Method

#### 3.1. Data

MODIS MOD09GA is an estimated surface reflectance product without consideration of atmospheric absorption and scattering and developed by the National Aeronautics and Space Administration (NASA) MODIS land product group following a unified algorithm. With a spatial resolution of 500 m and a temporal resolution of 1 day, MODIS MOD09GA data provide 7 bands in the Sinusoidal projection, including red band (Band 1, 0.62~0.67  $\mu\text{m}$ ), near infrared band (Band 2, 0.84~0.88  $\mu\text{m}$ ), blue band (Band3, 0.46~0.48  $\mu\text{m}$ ), green band (Band 4, 0.55~0.57  $\mu\text{m}$ ), shortwave infrared 1 band (Band 5, 1.23~1.25  $\mu\text{m}$ ), shortwave infrared 2 band (Band 6, 1.63~1.65  $\mu\text{m}$ ) and shortwave infrared 3 band (Band 7, 2.11~2.16  $\mu\text{m}$ ). In this study, MODIS MOD09GA data were adopted to evaluate the accuracy of different methods to identify lake ice during the freeze period (21 December 2019), complete freeze period (17 February 2018), ablation period (26 March 2017) and complete ablation period (6 April 2018) of Qinghai Lake, which were downloaded from NASA's Land Surface Distributed Data Center (<https://data.giss.nasa.gov> (accessed on 1 February 2020)). Furthermore, a total of nine scenes of Landsat ETM+ images and eight scenes of Landsat OLI images (Table 1) obtained from the United States Geological Survey (USGS) website (<http://glovis.usgs.gov> (accessed on 1 February 2020)) were used to assess the accuracy of the lake ice extraction method considering its higher spatial resolution of 30 m. To ensure the accuracy of the validation data, all these Landsat ETM+/OLI images are clear enough and with low cloud and snow cover to clearly show the distribution of lake ice on Qinghai Lake.

**Table 1.** Information of Landsat ETM+/OLI images.

ID	Sensor	Path/Row	Date	ID	Sensor	Path/Row	Date
01	ETM+	133/034	21 December 2019	10	OLI	133/034	26 March 2017
02	ETM+	133/035	21 December 2019	11	OLI	133/035	26 March 2017
03	ETM+	133/034	17 February 2018	12	OLI	134/036	24 April 2019
04	ETM+	133/035	17 February 2018	13	OLI	138/039	3 May 2018
05	ETM+	133/034	6 April 2018	14	OLI	138/039	1 March 2017
06	ETM+	133/035	6 April 2018	15	OLI	138/039	25 March 2019
07	ETM+	134/036	6 December 2017	16	OLI	136/034	31 March 2017
08	ETM+	134/036	15 May 2018	17	OLI	136/034	29 November 2018
09	ETM+	136/034	7 December 2018				

#### 3.2. Methods

Studies of Arctic sea ice have shown that the surface reflectance on sea water is consistently lower than that on sea ice, which is also true for lake ice and lake water [33]. The methods of lake ice identification based on optical images can be mainly summarized as the threshold method and the index method. The threshold method, which distinguishes between lake water and lake ice based on the difference of factors such as reflectance, temperature and backscatter coefficient, can be divided into the single-band threshold method and multi-band threshold method. Based on the fact that the reflectance of pure water tends to be almost zero while the ice reflectance is high in the near infrared band, the Single Band Threshold (SBT) method was used earlier to quickly monitor the changes in lake ice, but only small amounts of information on the band could be used [23]. The calculation formula is as follows:

$$\rho_{Nir} > T1 \quad (1)$$

where  $\rho_{Nir}$  represents the reflectance of the near infrared band, corresponding with MODIS MOD09GA band 2, and  $T1$  is the threshold, i.e., the pixels with reflectance greater than  $T1$  in the near infrared band are categorized as lake ice.

The reflectance difference threshold (RDT) method sets thresholds for the difference between the reflectance of the red and near infrared bands and the reflectance of the red

band to distinguish between lake water and lake ice, respectively, which not only can improve the extraction effect by using the interrelationship between different bands but also can eliminate certain atmospheric effects and errors, so it is more widely used in lake ice extraction studies [13,16]. Its calculation formula is as follows:

$$RDT = \begin{cases} \rho_{Red} - \rho_{Nir} > T2 \\ \rho_{Red} > T3 \end{cases} \quad (2)$$

where  $\rho_{Red}$  and  $\rho_{Nir}$  denote the reflectance of MOD09GA data in the red and near infrared bands, respectively, and  $T2$  and  $T3$  are the thresholds. When the reflectance difference between the red band and near infrared band is greater than  $T2$  and the reflectance of the red band is greater than  $T3$ , the pixel would be classified as lake ice.

Based on the analysis of the spectral characteristics of lake water and lake ice, the index method is able to construct different index models by synergizing multiple bands to realize the extraction of lake ice information. Based on the fact that the reflectance of snow and ice in the visible light band is much higher than that in the shortwave infrared band, the Normalized Difference Snow Index (NDSI) is one of the most common methods used to monitor snow [34]. It has also been applied to lake ice and sea ice monitoring [23,24]. Its calculation formula is as follows:

$$NDSI = \frac{\rho_{Green} - \rho_{SWIR2}}{\rho_{Green} + \rho_{SWIR2}} > T4 \quad (3)$$

where  $\rho_{Green}$  and  $\rho_{SWIR2}$  denote the reflectance of MOD09GA data in the green and shortwave infrared 2 bands, respectively, and  $T4$  is the threshold. When the NDSI value is greater than  $T4$ , the pixel would be classified as lake ice.

Some scholars have improved the NDSI method to obtain better data products [35,36]. For example, Wei et al. (2015) proposed the Modified Normalized Difference Snow Index (MNDSI) by replacing the green band of NDSI with the near infrared band. The difference between the MNDSI of lake ice and lake water is greater than their NDSI, as shown by the greater peak distance on the histogram and easier threshold setting. The calculation formula is as follows:

$$MNDSI = \frac{\rho_{Nir} - \rho_{SWIR2}}{\rho_{Nir} + \rho_{SWIR2}} > T5 \quad (4)$$

where  $\rho_{Nir}$  and  $\rho_{SWIR2}$  denote the reflectance of MOD09GA data in the near infrared band and shortwave infrared 2 band, respectively, and  $T5$  is the threshold. When the MNDSI value is greater than  $T5$ , the pixel would be classified as lake ice.

Based on the feature that the reflectance difference between lake water and lake ice is the largest in the red band, Li et al. (2018) introduced the red band on the basis of NDSI to propose the Lake Ice Index (LII) method, which improves the monitoring effect of lake ice by expanding the spectral difference between lake ice and lake water [37]. The calculation formula is as follows:

$$LII = \frac{\rho_{Red} \times (\rho_{Green} - \rho_{SWIR2})}{\rho_{Green} + \rho_{SWIR2}} > T6 \quad (5)$$

where  $\rho_{Red}$ ,  $\rho_{Green}$  and  $\rho_{SWIR2}$  refer to the reflectance of the red, green and shortwave infrared 2 bands, respectively, corresponding with MODIS MOD09GA band 1, band 4 and band 6, and  $T6$  is the threshold.

MODIS MOD09GA images covering Qinghai Lake on 26 March 2017 have good quality and similar lake ice and lake water areas and were selected to set 50 sample points of lake water and lake ice each uniformly (Figure 1). The index values of each sample point were calculated using the above methods and sorted in ascending order to directly reflect the range of the values (Figure 2). The results show that the values of each index of the lake ice sample points are usually larger than those of the lake water. The near infrared band reflectance (Figure 2a), red band reflectance (Figure 2b), the difference between red and near infrared band reflectance (Figure 2c) and LII values (Figure 2f) of lake water sample

points are concentrated in the low value interval, and suitable thresholds can be selected to distinguish them from the lake ice. The mean, maximum and minimum values of NDSI for lake ice sample points are 0.813, 0.919 and 0.472, respectively, while the three values for lake water sample points are 0.522, 0.805 and 0.073 (Figure 2d). Among them, the NDSI values of 17 lake ice sample points are less than the maximum value of lake water sample points, while the value of one lake ice sample point is even lower than the average value of lake water samples, causing a threshold of difficulty to be set in distinguishing water and ice. The improved MNDSI and LII methods expand the differences between the two categories of lake water and lake ice. The MNDSI values of lake water and lake ice range from  $-1$  to  $0.439$  and  $0.376$  to  $0.888$ , respectively. There is only one lake ice sample point with an MNDSI value smaller than the maximum value of the lake water sample point (Figure 2e). After introducing the red band into NDSI, the maximum and minimum values of LII for the lake ice sample point are  $0.393$  and  $0.085$ , respectively; the maximum and minimum values of LII at the lake water sample point are  $0.026$  and  $0.002$ , respectively; and the minimum value of LII at the lake water sample point is greater than the maximum value at the lake ice sample point. The above results show that it is difficult to separate lake water and lake ice by setting a threshold when using the NDSI method, but other methods can classify lake water and lake ice by selecting appropriate thresholds.

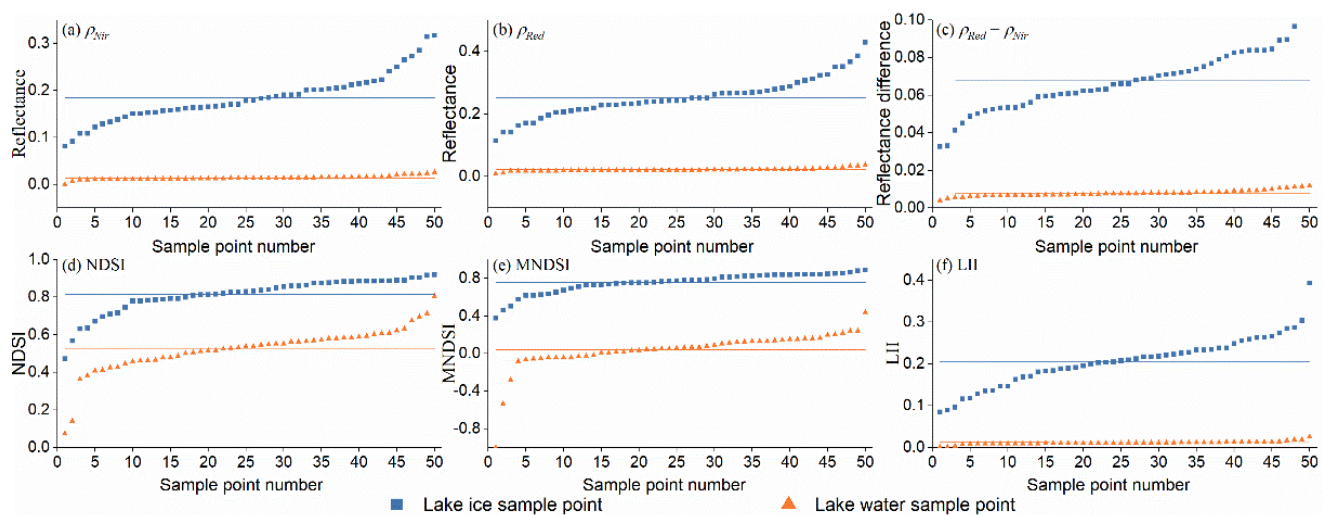


**Figure 2.** Index values of lake water and lake ice sample points of Qinghai Lake. (a)  $\rho_{Nir}$ ; (b)  $\rho_{Red}$ ; (c)  $\rho_{Red} - \rho_{Nir}$ ; (d) NDSI; (e) MNDSI; (f) LII.

Referring to the thresholds used in the existing studies, the above five methods were combined with the iterative threshold method to extract lake ice, and the extraction results of multiple iterative thresholds were compared with the visual interpretation results of Landsat images on the same day to determine the best threshold. The thresholds for lake ice extraction by each method in this study are listed in Table 2:

**Table 2.** Thresholds of optical remote sensing monitoring methods for lake ice used in this study.

Method	SBT	RDT			NDSI	MNDSI	LII
Threshold	T1 0.04	T2 0.028	T3 0.05	T4 0.65	T5 0.47	T6 0.07	

### 3.3. Accuracy Evaluation

Metrics for evaluating accuracy, including accuracy, precision, recall and mean intersection over union (MIoU), were selected to quantitatively assess the performance of the above remote sensing methods for extracting lake ice. Accuracy refers to the ratio of the

number of correctly predicted samples to the total number of samples. Precision refers to the ratio of correctly predicted lake ice pixels to the total number of pixels predicted to be lake ice, which can reflect whether the pixels are misidentified. Recall refers to the proportion of correctly predicted lake ice pixels to the total number of all actual lake ice pixels, reflecting whether the pixels are missed. MIoU refers to the mean of the ratio of the intersection and union of the true and predicted values for each category. The calculation formulas are as follows:

$$Accuracy = \frac{TP + TN}{TP + TN + FP + FN} \quad (6)$$

$$Precision = \frac{TP}{TP + FP} \quad (7)$$

$$Recall = \frac{TP}{TP + FN} \quad (8)$$

$$MIoU = \frac{1}{k + 1} \sum_{i=0}^k \frac{TP}{FN + FP + TP} \quad (9)$$

where  $TP$  refers to the number of pixels correctly predicted as lake ice,  $FP$  refers to the number of pixels incorrectly predicted as lake ice,  $FN$  refers to the number of pixels incorrectly predicted as lake water,  $TN$  refers to the number of pixels correctly predicted as lake water, and  $k$  is the number of classes.

## 4. Results

### 4.1. Comparison of the Percentage of Lake Ice Area Extracted by Different Remote Sensing Monitoring Methods

Usually, the percentage of lake ice area to total lake area (such as 5% or 95%) is used to determine the beginning date of freezing, complete freezing, melting and complete melting of the lake, serving as an important parameter for identifying phenological events of lake ice [38]. To evaluate the benefits and drawbacks of different optical-image-based lake ice extraction methods, the percentages of lake ice area from these methods were compared with the true values (Table 3), which were visually interpreted in the freeze, complete freeze, ablation and complete ablation periods of Qinghai Lake from Landsat ETM+/OLI images.

**Table 3.** Errors of lake ice area percentages in Qinghai Lake extracted by different monitoring methods in different periods.

	Date	True Value of the Percentage of Lake Ice Area (%)	Absolute Values of Percentage Error of Lake Ice Area Extracted by Different Methods (%)				
			LII	RDT	SBT	NDSI	MNDSI
Freeze period	21 December 2019	18.09	3.92	5.90	1.81	4.33	6.09
complete Freeze period	17 February 2018	100.00	1.02	1.99	0.00	4.19	12.67
Ablation period	26 March 2017	45.09	0.10	0.73	7.59	5.04	0.10
complete Ablation period	6 April 2018	2.09	1.07	0.31	2.12	1.12	0.53
mean	-	-	1.53	2.23	2.88	3.67	4.85

As seen from Table 3, in the freeze period of Qinghai Lake, the SBT method has the best monitoring results, and the monitoring error of the lake ice area percentage is 1.81%, followed by the LII method and the NDSI method, with errors of 3.92% and 4.33%, respectively, while the RDT and MNDSI methods perform the worst, with errors of 5.90% and 6.09%. During the complete freeze period of Qinghai Lake, the SBT method still gives the best result. The errors of the LII method, the RDT method and the NDSI method are 1.02%, 1.99% and 4.19%, respectively, while the MNDSI method gives the worst monitoring result with an error of up to 12.67%. During the ice ablation period of Qinghai Lake, the LII method and MNDSI method yield better monitoring results with an error

of 0.10% for both; the second is the RDT method with an error of 0.73%, while the SBT method, which has the best result during the freezing period, produces the largest error (7.59%). In the complete ablation period of Qinghai Lake, the monitoring results of five methods are indifferent. The errors ranging from low to high are the RDT, MNDSI, LII, NDSI and SBT method. Overall, the LII method has the smallest averaged monitoring error (1.53%), followed by the RDT method (2.23%), SBT method (2.88%), NDSI method (3.67%) and MNDSI method (4.85%). Compared with the NDSI method and the MNDSI method, the LII method has an obviously improved accuracy of lake ice extraction, especially during the freeze period and the complete freeze period. Although the SBT method has better monitoring results during the freezing process, the errors during the ablation and complete ablation periods are greater than the other four methods. Interestingly, the monitoring performance of the RDT method is roughly opposite to that of the SBT method. Therefore, from the perspective of the entire freezing–thawing process of Qinghai Lake, the LII method performs the best in the extraction of lake ice, which can effectively improve the accuracy of lake ice phenology information.

#### 4.2. Comparison of the Spatial Accuracy of Different Methods to Identify Lake Ice

The accuracy of lake ice location identification is also important to evaluate different extraction methods. To evaluate the accuracy of different methods in this aspect, with the visual interpretation results of Landsat ETM+/OLI images in different periods as true values, the extraction results of various lake ice monitoring methods based on MODIS MOD09GA images were compared (Figure 3). The confusion matrix was obtained based on the classification results of each remote sensing method and the accuracy, precision, recall and MIoU were further calculated to evaluate the classification accuracy (Table 4).

**Table 4.** Performance comparison of different lake ice remote sensing extraction methods.

Date	Method	Evaluation Indicator			
		Accuracy (%)	Precision (%)	Recall (%)	MIoU (%)
21 December 2019	LII	92.56	88.00	68.31	77.00
	RDT	91.46	89.58	59.88	73.20
	SBT	93.05	84.93	74.73	77.97
	NDSI	88.35	73.81	55.98	66.86
	MNDSI	90.07	67.00	89.07	75.03
17 February 2018	LII	98.92	100.00	98.92	49.46
	RDT	96.71	100.00	96.71	48.36
	SBT	100.00	100.00	100.00	100.00
	NDSI	95.83	100.00	95.83	47.92
	MNDSI	87.33	100.00	87.33	43.67
26 March 2017	LII	89.91	87.83	89.73	83.07
	RDT	89.82	87.95	89.36	81.36
	SBT	86.15	81.81	88.51	75.56
	NDSI	82.94	80.10	81.98	70.64
	MNDSI	86.51	84.24	85.67	76.02
6 April 2018	LII	98.89	90.37	48.56	72.53
	RDT	98.35	61.22	56.00	69.84
	SBT	95.61	29.13	78.13	61.23
	NDSI	96.49	24.73	39.08	57.15
	MNDSI	99.06	82.37	65.80	78.36

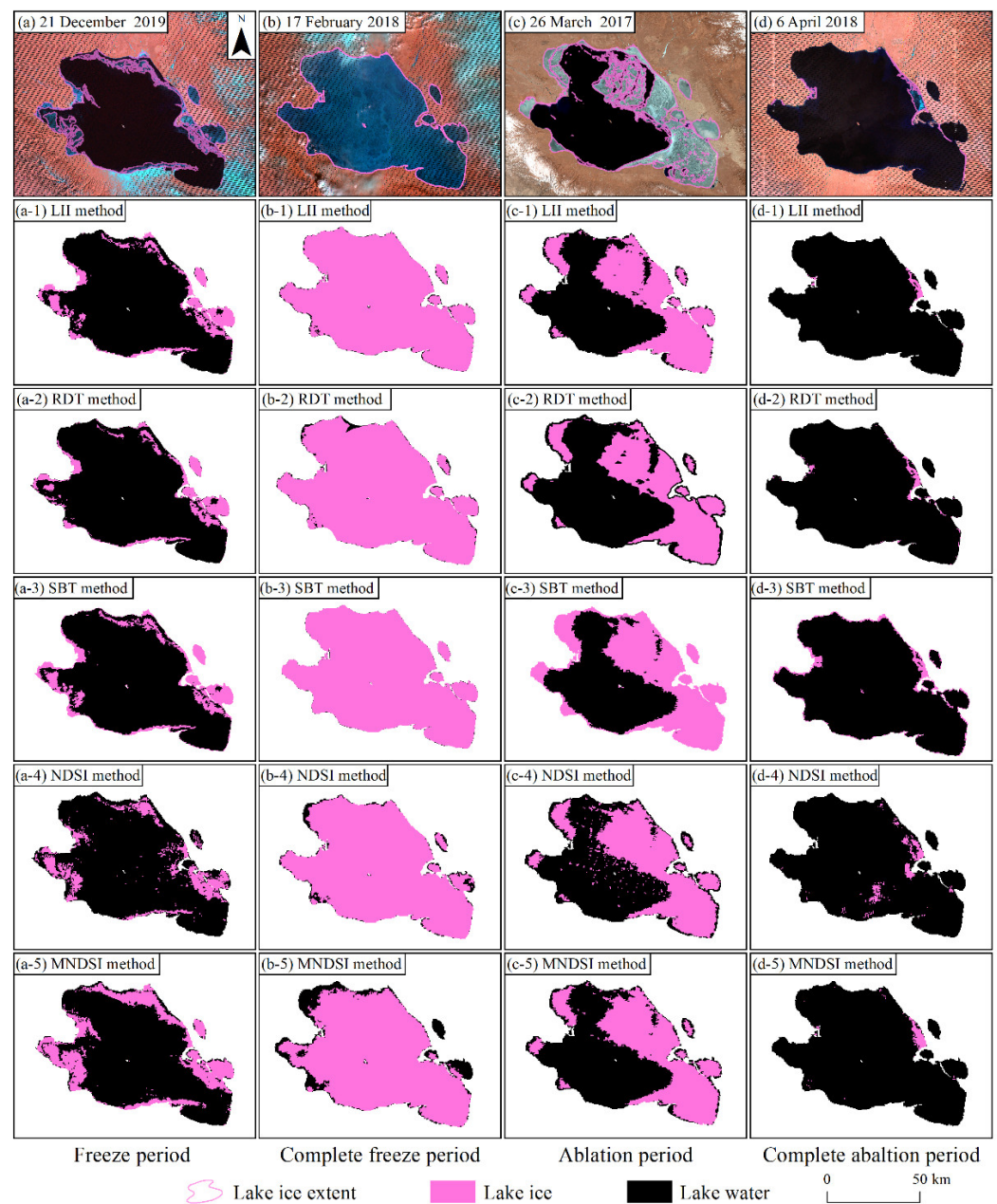


**Figure 3.** Distributions of lake ice of Qinghai Lake by different monitoring methods for Landsat ETM+ images accessed on 21 December 2019 (a–a-5) and 17 February 2018 (b–b-5), Landsat OLI images accessed on 26 March 2017 (c–c-5), and Landsat ETM+ images accessed on 6 April 2018 (d–d-5).

The Landsat ETM+ image on 21 December 2019 shows that Qinghai Lake has entered the freeze period, with 18.09% of the total lake freezing as ice, mainly in the southern margin part of the lake with snow cover (Figure 3a). The SBT method has the smallest percentage error for the lake ice area, with accuracy, precision, recall and MIoU of 93.05%, 84.93%, 74.73% and 77.97%, respectively. It has a strong ability to monitor broken ice on the north of the lake but misidentifies a small portion of lake water at the water-land junction (e.g., at the lake center island) as lake ice and also misses some thin ice pixels in Haiyan Bay (Figure 3(a-3)). The LII method and the RDT method mainly fail to detect the broken lake ice on the north and west of the lake, as well as the thin ice in Haiyan Bay (Figure 3(a-1,a-2)). Correspondingly, the precision of the SBT method is 3.07% and 4.65% smaller than that of the LII method and RDT method, respectively, while its recall is 6.42% and 14.85% higher than the latter two, respectively. The NDSI method can only identify thick ice with high

brightness and misjudges the scattered lake water pixels in the middle of the lake as lake ice (Figure 3(a-4)). The accuracy, precision, recall and MIoU of LII method increased by 4.21%, 14.19%, 12.33% and 10.14%, respectively, compared to the NDSI method, indicating that the LII method performs better than the NDSI method. The MNDSI method can correctly classify most of the pixels in the middle of the lake, but the pixels at the junction of the broken ice and water in the north are identified as continuous large pieces of lake ice, causing lower accuracy and the largest error of lake ice area percentage (Figure 3(a-5)).

The Landsat ETM+ image on 17 February 2018 shows that Qinghai Lake was completely frozen, with small patches of lake ice covered by snow in the northern part of the lake and a few scattered thick clouds in the southwest corner (Figure 3b). The actual classification of all the pixels is lake ice, so the lake ice pixels predicted by each method are correctly classified. In addition, the precision of the extraction result of each method is 1. The difference between the extraction results of the five methods is mainly represented by the recall, where a larger recall means that fewer lake ice pixels are missed. The SBT method has the highest accuracy and is able to detect all lake ice, so the recall is 100% (Figure 3(b-3)). In addition, the LII method extracted lake ice better with 98.92%, 100.00%, 98.92% and 49.46% values for accuracy, precision, recall and MIoU, respectively. Both the LII method and the NDSI method are affected by cloud and fail to detect the lake ice beneath it. The LII method is more affected by the thick clouds in the southwest corner, while the NDSI method also has a poor performance in monitoring the lake ice under thin cloud in Haiyan Bay (Figure 3(b-1,b-4)). The RDT method is affected by snow cover and cannot detect the small amount of lake ice in the north (Figure 3(b-2)). The MNDSI method has poor monitoring effects under clouds and at the water–land junction, with the lowest accuracy (87.33%) and the largest monitoring error of 12.67% in the percentage of lake ice area (Figure 3(b-5)).

On 26 March 2017, Qinghai Lake already entered the ablation period, with 45.09% of the lake ice area. Large patches of firm lake ice are mainly located in the eastern part of the lake, followed by the western part, with large amounts of water occupying the central region of the lake, accompanied by broken lake ice (Figure 3c). Influenced by the mixing ice and water, uneven thickness of lake ice and the spatial resolution of remote sensing images, none of the five methods can extract details of lake ice. Among them, the LII and MNDSI methods have the smallest error in monitoring the percentage of lake ice area (Figure 3(c-1,c-5))—both at 0.1%. However, the MNDSI method fails to identify the lake ice on the lake shore, so its recall is 4.06% lower than that of the LII method. It also misjudges part of lake water pixels on the northern of the lake as lake ice, so its precision is 3.59% lower than that of the LII method. As a result, the MNDSI method wrongly identifies the lake water pixels in the northern part of Qinghai Lake as lake ice, and these misidentified lake ice areas compensate for some of the missed lake ice areas at the lake shore, resulting in a final lake ice area close to the true value. In fact, the location of the lake ice pixels predicted by the MNDSI method is not accurate, with an accuracy 3.4% lower than that of the LII method. The SBT method, which performs better in the freezing process, shows the largest error of 7.59% in lake ice area percentage at this time, with accuracy, precision, recall and MIoU of 86.15%, 81.81%, 88.51% and 75.56%, respectively, which are smaller than the evaluation metrics of the LII method.

On 6 April 2018, most of the lake ice in Qinghai Lake already melted completely, and only a small amount of lake ice existed on the west and east shores of the lake (Figure 3d). The accuracies of all five methods were greater than 95%, among which the LII (accuracy = 98.89%, precision = 90.37%, recall = 48.56%, MIoU = 72.53%) and MNDSI methods (accuracy = 99.06%, precision = 82.37%, recall = 65.08%, MIoU = 78.36%) are more effective in monitoring. Compared to the other four methods, the MNDSI method has the best extraction effect on the lake ice on the eastern bank (Figure 3(d-5)). The LII method (Figure 3(d-1)), RDT method (Figure 3(d-2)) and MNDSI method work well for lake ice on the west shore. The SBT method misclassifies some lake water near the lake shore (Figure 3(d-3)), and the NDSI method misclassifies the lake water on the north-

east and south of Qinghai Lake (Figure 3(d-4)), both with low precisions of 29.13% and 24.73%, respectively.

Although the errors of lake ice area percentages of the SBT method and the RDT method are relatively small, the former has a poor ability to distinguish lake ice at the water–land junction, and the latter has poor recognition ability in snow-covered areas. In contrast, the LII method not only has smaller errors in the percentage of lake ice area throughout the freeze–thaw cycle but also has relatively higher accuracy, precision, recall and MIoU. In addition, the accuracy of the LII method is consistently greater than that of the NDSI method and MNDSI method, which indicates that the extraction results have been improved. Overall, the LII method is more powerful in identifying lake ice pixels.

#### 4.3. Influence of Snow Cover on Lake Ice Extraction Results

Snow cover is one of the important phenomena on the surface of the lake during the cold season and may have an impact on the lake ice monitoring. The Landsat ETM+ image covering Qinghai Lake on 22 January 2020 (only 4% of the entire image is cloudy) shows that the lake is completely frozen with large amount of snow on the lake surface. Based on the MODIS MOD09GA image of Qinghai Lake on that date, we calculated the percentage error of the lake ice area extracted by each of the above five lake ice remote sensing monitoring methods to analyze the possible impact of snow on lake ice monitoring (Figure 4). The results show that when the lake ice surface is covered by snow, the SBT method and LII method both have the smallest monitoring error (0%), followed by the MNDSI method (0.43%) and the NDSI method (0.89%). The RDT method has the worst monitoring performance, with an error of 53.72% (Figure 4f). According to the principle of lake ice discrimination of the RDT method, when the difference between  $\rho_{Red}$  and  $\rho_{Nir}$  is greater than 0.02 and  $\rho_{Red}$  is greater than 0.05, the pixel is recognized as lake ice. However, the former value of the snow-covered lake ice pixels is less than 0.02 (Figure 4g), and the latter is greater than 0.05 (Figure 4h), which does not satisfy the requirements for identifying it as lake ice. Therefore, the RDT method is most affected by snow cover. If the RDT method is used to extract lake ice, attention should be paid to the choice of threshold values (especially the a-value) in the case of snow presence.

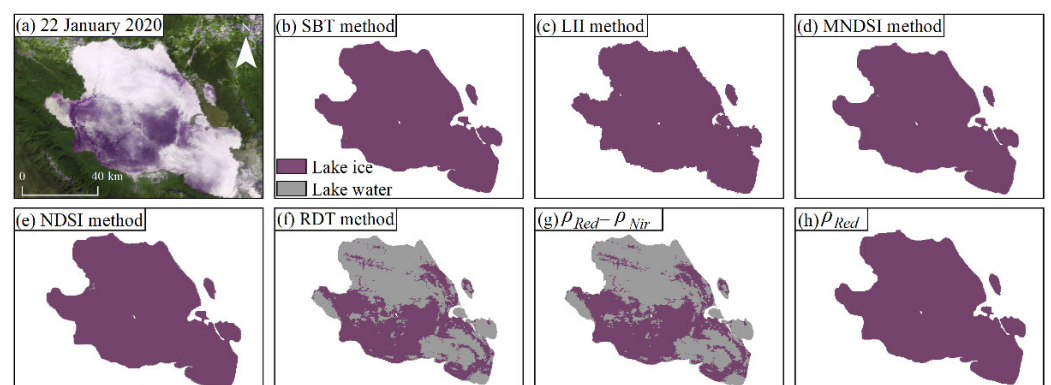


**Figure 4.** Ice extent of Qinghai Lake extracted by different monitoring methods under snow-covered scenes. (a) MODIS MOD09GA image on 22 January 2020, and the composite band is 1-2-3; (b) SBT method; (c) LII method; (d) MNDSI method; (e) NDSI method; (f) RDT method; (g)  $\rho_{Red} - \rho_{Nir}$ ; (h)  $\rho_{Red}$ .

## 5. Discussion

Global lake warming is occurring at a higher rate than the atmosphere and oceans [39]. Given the background, the reduction in ice-free periods, the large loss of northern hemisphere lake ice areas and the thinning of ice thickness suggest a threatened future for ice cover [40–43]. Alpine lakes in mid-latitude (e.g., in Mediterranean) and high-altitude (e.g., in the Tibetan Plateau) regions are less affected by human activities, and their winter ice

cover characteristics are sensitive to climate change. For example, Cai et al. found that the variation in ice cover duration showed a large spatial heterogeneity based on the ice phenology records of 71 lakes on the Tibetan Plateau between 2001 and 2020, and that climate factors represented by temperature and solar radiation were the main causes of this phenomenon [44]. Caldwell et al. found that snow fraction and air temperature are the strongest predictors of ice break-up and predicted that the lake ice melt date in mountain lakes would be tens of days earlier by the end of the century [45]. Ice thickness is also one of the important properties of the ice cover and is mainly determined by temperature, precipitation and the thickness of the snow covering on it [46,47]. Winter limnology studies have revealed that ice cover can obstruct the source of dissolved oxygen in lakes (oxygenated photosynthesis and exchange with the atmosphere), leading to oxygen depletion in winter, and changes in lake ice phenology and ice thickness in response to climate would have an impact on lake ecosystems [48–50]. Although the study of lake ice phenology has become one of the topics of great interest [22], most attention has been focused on high latitudes, with only few data and little knowledge regarding mid-latitude alpine lake ice cover [46,47,49]. Long-term accurate lake ice phenology data are the basis for exploring lakes in winter. Remote sensing is currently the most commonly used method for lake ice phenology extraction. The selection of accurate and stable lake ice extraction methods is one of the important prerequisites for conducting lake ice phenology research, so it is necessary to analyze the advantages and disadvantages of common lake ice remote sensing monitoring methods. In this study, the SBT, RDT, NDSI, MNDSI and LII methods based on MODIS MOD09GA data were used to extract lake ice in different ice periods of Qinghai Lake, and the classification results were evaluated based on the error of the percentage of lake ice area, combined with four evaluation metrics of accuracy, precision, recall and MIoU. The above results suggest that the extraction results of the latest proposed LII method have higher accuracy throughout the freeze–thaw cycle.

### 5.1. Validation of LII Method for Detecting Long-Term Lake Ice Phenology Dates in Qinghai Lake

In view of the above results, the LII method was used to extract the long time series of lake ice phenology dates of Qinghai Lake, and a comparison was made with the results of previous studies on the freeze–thaw dates of Qinghai Lake from 2000 to 2016 based on the RDT method [31] and passive microwave remote sensing data [17]. Taking the lake ice area accounting for 10% and 90% of the whole lake area as the criterion, the lake ice phenological data of Qinghai Lake from 2000 to 2016 were extracted using the LII method (the threshold was 0.07) (Figure 5). The results show that the lake freeze-up starting date (FUS) extracted by the RDT method and the LII method had the highest consistency, with the largest correlation coefficient ( $R^2 = 0.95$ ) and the smallest mean absolute error (MAE = 1.56 days), while the FUS obtained based on passive microwave remote sensing data was generally later than the LII method ( $R^2 = 0.68$ , MAE = 4.19 days) (Figure 5a). For the freeze-up ending date (FUE), the extract results of the RDT method and passive microwave remote sensing images both showed the worst fits with the LII method, with  $R^2$  values of 0.70 and 0.65, respectively, and the FUE obtained from the passive microwave remote sensing data was obviously earlier than that of the LII method, with an MAE of 16.81 day (Figure 5b). For the break-up starting (BUS) date of the lake, the correlation of the extraction results between the LII method and passive microwave remote sensing images ( $R^2 = 0.87$ , MAE = 4.44 days) was lower than that between it and the reflectance difference method ( $R^2 = 0.91$ , MAE = 3.81 days) (Figure 5c). For the lake break-up ending date (BUE), the three methods have relatively high consistency. The  $R^2$  and MAE of the extraction results of the LII method with the RDT method and passive microwave remote sensing image are 0.86 and 3.13 days, 0.84 days and 3.69 days, respectively (Figure 5d). Therefore, the two methods based on MODIS images have strong consistency in extracting lake ice phenology dates in general. The results extracted from passive microwave remote sensing images are more similar to the LII method in the lake ice ablation process, while the FUE obtained by the former is generally earlier than the results obtained by the LII

method, and the FUS and BUE mostly lag behind the latter. This phenomenon is mainly attributed to the freeze–thaw spatial pattern of Qinghai Lake, the rough spatial resolution of passive microwave remote sensing images and the different methods of extracting lake ice from the two data sources [17,51]. At first, the spatial pattern of freezing and melting in Qinghai Lake is characterized by shallow water on the lake shore freezing/melting first and then expanding towards the center of the lake. Secondly, the spatial resolution of passive microwave remote sensing images is poor, and only pixels close to the center of the lake are considered as available pixels to avoid the influence of mixed pixels, so these central pixels can only represent the freeze–thaw information in the center of the lake. For FUS, the higher spatial resolution of optical remote sensing imagery allows for the timely detection of lake shore freezing. The date when the lake ice expands towards the center until the bright temperature of passive microwave remote sensing pixels change significantly will be later. Similarly, when Qinghai Lake starts to melt, the small amount of already melted lake ice on the lake shore has little effect on the passive microwave pixels in the center of the lake, so the BUS determined by the LII method is usually earlier. When determining the FUE date based on the variation of the brightness temperature curve, the date when the brightness temperature rises to a stable peak is usually chosen as the result. However, there is actually a small rising phase in the brightness temperature after reaching the stable peak, which is not yet determined whether it is caused by the incomplete freezing of the lake ice or the increase of the lake ice thickness after complete freezing. In addition to the spatial resolution, this could be another error source of FUE [17].

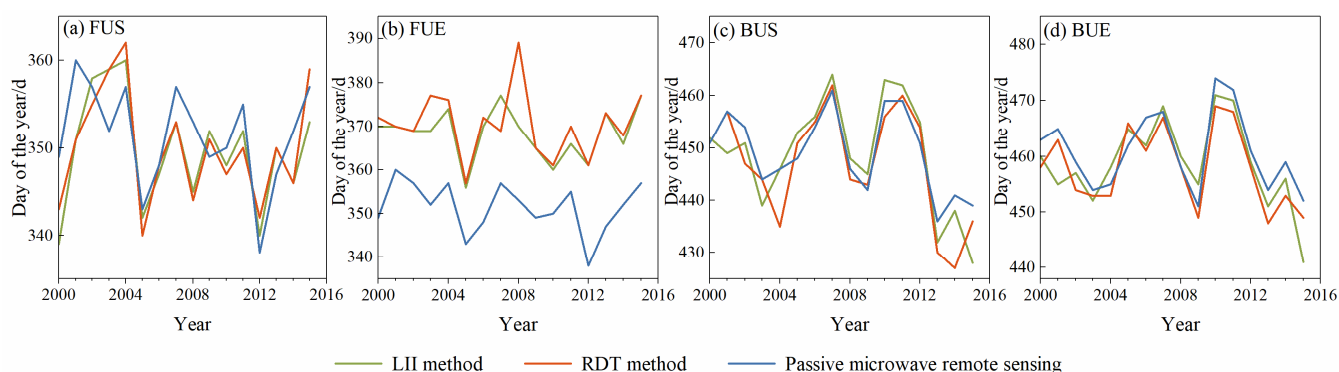


**Figure 5.** Comparison of the lake ice phenology of Qinghai Lake from 2000 to 2016 based on passive microwave remote sensing data, the RDT method and the LII method. (a) FUS; (b) FUE; (c) BUS; (d) BUE.

Cloud is one of the main error sources affecting the extraction of lake ice phenology based on MODIS MOD09GA data. We counted the number of days affected by clouds when extracting the long-term lake ice phenology of Qinghai Lake, and the results showed that 16 out of the 64 lake ice phenology records of Qinghai Lake in 16 years were affected by clouds, with an average error of 2.5 days when extracted by the LII method, while the error affected by clouds in the extracted BUS was only 1 day, which occurred on 7 April 2011. From 6 to 11 January 2008, the FUE in this freezing period could not be accurately judged due to the influence of clouds, resulting in the maximum observation error of 6 day. Although cloud cover affects the accuracy of identifying the location of lake ice, the advantage of the high temporal resolution of MODIS MOD09GA data can still provide some reference for the accurate judgment of lake ice phenology characteristics. Therefore, lake ice phenology dates calculated based on MODIS data were usually used as validation data to evaluate results obtained based on other remote sensing data or models in previous studies. Although the differences in data and methods lead to inconsistencies in the actual obtained dates of lake ice freezing and thawing, there is still a high correlation between the results obtained from different remote sensing data [51]. In our opinion, in addition to considering the elimination of the influence of clouds on optical remote sensing

images or expanding the application of passive microwave remote sensing images through mixed pixel decomposition, it is also feasible to integrate the results from different data sources based on their high consistency.

### 5.2. Adaptability of LII Method

There are numerous and widely distributed lakes on the QTP, where the characteristics (such as salinity and suspended particulate matter) of lake water vary from lake to lake, and the distribution of bubbles and ice thickness are not consistent in different ice periods, which is reflected in the images as the difference in the optical properties of water and ice. For example, during the early freezing and late thawing periods, lake ice thins and mixes with water, featured by low reflectance, which is similar to the optical properties of lake water and makes it difficult to be identified. In addition, when the density of suspended solids and chlorophyll in the water is very high after the lake ice melts, the reflectance of the water body increases, and the peak value moves to the long-wave direction (from blue to green band), which brings difficulties for classification [20]. Furthermore, when using the index method for classification, the rationality of the threshold is also one of the important conditions affecting the classification accuracy. Therefore, it is necessary to explore the applicability of lake ice remote sensing monitoring methods for various lakes and to determine reasonable thresholds.

To verify the applicability of the LII method for monitoring different types of lakes, a freshwater lake (Ngoring Lake), fresh-brackish water lake (Nam Co), brackish lake (Qinghai Lake) and saltwater lake (Xiao Qaidam Lake) located on the QTP were selected for testing. The qualified MODIS MOD09GA images in the freezing period, complete freeze period and ablation period were selected to calculate their LII values, respectively. Starting from 0, different thresholds for lake ice area extraction by the LII method were determined in steps of 0.01. Then, the percentage error of the lake ice area extracted based on each threshold is calculated (Figure 6). During the freeze period and the ablation period (the green and red lines in Figure 6), the percentage errors of the lake ice area of the four types of lakes decrease first and then increase with the increase of the threshold, and finally stabilize at the maximum value. When the lake is completely frozen (the blue line in Figure 6), the lake surface is completely covered by ice. The percentage errors of the lake ice area of the four types of lakes increase with rising threshold and remain unchanged after reaching 100%. Although the thresholds corresponding to the minimum monitoring errors of four types of lakes in the three periods are different, they are basically between 0.05 and 0.07. The largest error (5.834%) in this interval appears in the freeze period of Nam Co, with a threshold of 0.07. When the thresholds are 0.05, 0.06 and 0.07, the average monitoring errors of the four types of lakes in the three ice periods are 3.21%, 3.08% and 3.43%, respectively, indicating that the LII method performs well in monitoring the extent of lake ice based on this threshold range and has good universality for different types of lakes. Therefore, the threshold range of 0.05–0.07 can provide a reference for the rapid extraction of lake ice phenology for numerous lakes on the QTP using the LII method. In addition, for a specific lake, it is necessary to select the optimal threshold within the empirical threshold range to ensure the accurate extraction of lake ice area. These findings can provide a reference for further research of mid-latitude mountain lakes to determine their characteristics, drivers, future trends and impacts of ice phenology changes.

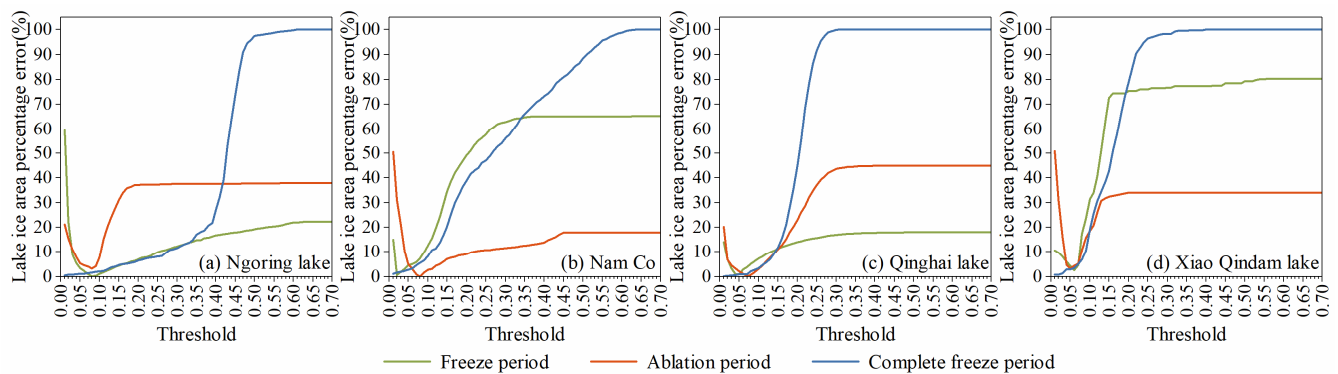


**Figure 6.** Variation of percentage error of lake ice area with LII threshold in Ngoring Lake (a), Nam Co (b), Qinghai Lake (c), Xiao Qindam Lake (d).

## 6. Conclusions

In this study, the performance of five optical remote sensing monitoring methods based on MODIS MOD09GA images for extracting the extent of lake ice were compared with Qinghai Lake as an example, and the ability of the LII method to extract long term lake ice phenology events and its applicability in large regional applications were further analyzed. The following main conclusions are drawn:

1. Among the five remote sensing monitoring methods, the near infrared band reflectance, red band reflectance and the reflectance difference between the red and near infrared band at the lake ice sample points are usually larger than that of lake water, indicating that both SBT and RDT methods can set suitable thresholds to distinguish lake water and lake ice. The NDSI values of some lake ice sample points are smaller than the NDSI values of lake water, which makes the threshold segmentation difficult. Both the MNDSI method and LII method, which are improved by the NDSI method, can increase the difference between lake water and lake ice and are more favorable to distinguish them.
2. The monitoring effect of the single band threshold method is better during the freezing period but worse during the ablation period, and that of the RDT method is poor during the freeze period and for snow-covered scenes. Compared with the NDSI method and the MNDSI method, the LII method is significantly more effective in monitoring the lake ice extent of Qinghai Lake during different periods. The LII method has the best monitoring effect in the entire lake freeze–thaw cycle and can be used to extract long-term lake ice phenology features of Qinghai Lake.
3. Both the RDT method and the LII method are based on MODIS images, and their extracted lake ice phenology records from 2000 to 2016 of Qinghai Lake are consistent. The FUE extracted based on passive microwave remote sensing imagery is overall earlier than that based on MODIS MOD09GA imagery, while BUE usually lags behind the latter. The mean error caused by cloud when extracting the lake ice phenology date using the LII method is 2.5 days.
4. The LII method is suitable for the extraction of the lake ice extent of different types of lakes such as freshwater lakes, brackish water lakes and salt lakes on the QTP. The reasonable threshold range of 0.05~0.07 is helpful to improve the efficiency of extracting lake phenology features in a large region.

**Author Contributions:** Conceptualization, H.Z. and X.Y.; Methodology, H.Z.; Supervision, X.Y.; Validation, Q.W., H.D. and Y.Z.; Writing—original draft, H.Z. All authors have read and agreed to the published version of the manuscript.

**Funding:** This research was funded by the National Natural Science Foundation of China (grant numbers 42071089, 41861013), National Key Research Program of China (grant number 2019YFE0127700) and the Northwest Normal University Graduate Research Grant Program (grant number 2020KYZZ001157).

**Data Availability Statement:** MODIS MOD09GA data are available at <https://data.giss.nasa.gov>, accessed on 1 February 2020 (NASA's Land Surface Distributed Data Center, 2020). Landsat ETM+/OLI data are available at <http://glovis.usgs.gov>, accessed on 1 February 2020 (USGS, 2020).

**Acknowledgments:** Thanks to the data providing platforms NASA's Land Surface Distributed Data Center (<https://data.giss.nasa.gov> (accessed on 1 February 2020)) and United States Geological Survey (<http://glovis.usgs.gov> (accessed on 1 February 2020)).

**Conflicts of Interest:** The authors declare no conflict of interest.

## References

1. IPCC. *Climate Change 2021: The Physical Science Basis. Contribution of Working Group I to the Sixth Assessment Report of the Intergovernmental Panel on Climate Change*; Cambridge University Press: Cambridge, UK; New York, NY, USA, 2021.
2. Verpoorter, C.; Kutser, T.; Seekell, D.A.; Tranvik, L.J. A global inventory of lakes based on high-resolution satellite imagery. *Geophys. Res. Lett.* **2014**, *41*, 6396–6402. [[CrossRef](#)]
3. Zhu, L.P.; Peng, P.; Zhang, G.Q.; Qiao, B.J.; Liu, C.; Yang, R.M.; Wang, J.B. The role of Tibetan Plateau lakes in surface water cycle under global changes. *J. Lake Sci.* **2020**, *32*, 597–608.
4. Zhu, L.P.; Ju, J.T.; Qiao, B.J.; Yang, R.M.; Liu, C.; Han, B.P. Recent lake changes of the Asia Water Tower and their climate response: Progress, Problems and Prospects. *Chin. Sci. Bull.* **2019**, *64*, 2796–2806. (In Chinese)
5. Assel, R.A.; Robertson, D.M. Changes in winter air temperatures near Lake Michigan, 1851–1993, as determined from regional lake-ice records. *Limnol. Oceanogr.* **1995**, *40*, 165–176. [[CrossRef](#)]
6. WMO. *Systematic Observation Requirements for Satellite-Based Products for Climate*; WMO/TD-No. 1338; GCOS-No. 107; WMO: Geneva, Switzerland, 2006; Volume 1338, p. 103.
7. Weber, H.; Riffler, M.; Nöges, T.; Wunderle, S. Lake ice phenology from AVHRR data for European lakes: An automated two-step extraction method. *Remote Sens. Environ.* **2016**, *174*, 329–340. [[CrossRef](#)]
8. Yu, M.; Lu, P.; Cao, X.W.; Tang, M.G.; Wang, Q.K.; Li, Z.J. Field observations of the bidirectional reflectance characteristics of lake ice. *Spectrosc. Spectral Anal.* **2020**, *40*, 2453–2461.
9. Wang, G.X.; Zhang, T.J.; Yang, R.M.; Zhong, X.Y.; Li, X.D. Lake ice changes in the Third Pole and the Arctic. *J. Glaciol. Geocryol.* **2020**, *42*, 124–139. [[CrossRef](#)]
10. Sharma, S.; Blagrove, K.; Watson, S.R.; O'Reilly, C.M.; Batt, R.; Magnuson, J.J.; Clemens, T.; Denfeld, B.A.; Flaim, G.; Grinberga, L.; et al. Increased winter drownings in ice-covered regions with warmer winters. *PLoS ONE* **2020**, *15*, e0241222. [[CrossRef](#)]
11. Sharma, S.; Meyer, M.F.; Culpepper, J.; Yang, X.; Hampton, S.; Berger, S.A.; Brousil, M.R.; Fradkin, S.C.; Higgins, S.N.; Jankowski, K.J.; et al. Integrating perspectives to understand lake ice dynamics in a changing world. *J. Geophys. Res. Biogeosci.* **2020**, *125*, e2020JG005799. [[CrossRef](#)]
12. Magnuson, J.J.; Robertson, D.M.; Benson, B.J.; Wynne, R.H.; Livingstone, D.M.; Arai, T.; Assel, R.A.; Barry, R.G.; Card, V.; Kuusisto, E.; et al. Historical trends in lake and river ice cover in the northern hemisphere. *Science* **2000**, *289*, 1743–1746. [[CrossRef](#)]
13. Wei, Q.F.; Ye, Q.H. Review of lake ice monitoring by remote sensing. *Prog. Geogr.* **2010**, *29*, 803–810.
14. Han, W.X.; Huang, C.L.; Gu, J.; Hou, J.L.; Zhang, Y. Spatial-Temporal distribution of the freeze-thaw cycle of the largest lake (Qinghai Lake) in China based on Machine Learning and MODIS from 2000 to 2020. *Remote Sens.* **2021**, *13*, 1695. [[CrossRef](#)]
15. Sun, H.; Li, C.H.; Yao, X.J. Extraction and analysis of lake ice in typical lakes on the northern slopes of the Himalayas based on NPP-VIIRS data. *J. Glaciol. Geocryol.* **2021**, *43*, 70–79.
16. Qi, M.M.; Liu, S.Y.; Yao, X.J.; Xie, F.M.; Gao, Y.P. Monitoring the ice phenology of Qinghai Lake from 1980 to 2018 using multisource remote sensing data and google earth engine. *Remote Sens.* **2020**, *12*, 2217. [[CrossRef](#)]
17. Cai, Y.; Ke, C.Q.; Duan, Z. Monitoring ice variations in Qinghai Lake from 1979 to 2016 using passive microwave remote sensing data. *Sci. Total Environ.* **2017**, *607*, 120–131. [[CrossRef](#)]
18. Wang, G.X.; Zhang, T.J.; Li, X.D.; He, Z.L.; Li, Y.X. Detecting changes of ice phenology using satellite passive microwave remote sensing data in Qinghai Lake. *J. Glaciol. Geocryol.* **2019**, *43*, 296–310.
19. Wakabayashi, H.; Motohashi, K.; Maezawa, N. Monitoring lake ice in Northern Alaska with backscattering and interferometric approaches using Sentinel-1 SAR data. In Proceedings of the IGARSS 2019—2019 IEEE International Geoscience and Remote Sensing Symposium, Yokohama, Japan, 28 July 2019; pp. 4202–4205.
20. Heinilä, K.; Mattila, O.; Metsämäki, S.; Väkevä, S.; Luojus, K.; Schwaizer, G.; Koponen, S. A novel method for detecting lake ice cover using optical satellite data. *Int. J. Appl. Earth Obs. Geoinf.* **2021**, *104*, 102566. [[CrossRef](#)]
21. Reed, B.; Budde, M.; Spencer, P.; Miller, A.E. Integration of MODIS-derived metrics to assess interannual variability in snowpack, lake ice, and NDVI in southwest Alaska. *Remote Sens. Environ.* **2009**, *113*, 1443–1452. [[CrossRef](#)]
22. Murfitt, J.; Duguay, C.R. 50 years of lake ice research from active microwave remote sensing: Progress and prospects. *Remote Sens. Environ.* **2021**, *264*, 112616. [[CrossRef](#)]
23. Gou, P.; Ye, Q.H.; Wei, Q.F. Lake ice change at the Nam Co Lake on the Tibetan Plateau during 2000–2013 and influencing factors. *Prog. Geogr.* **2015**, *34*, 1241–1249.
24. Zhangxin, E.D.C. Using the sea ice data of MODIS to inspect the seasonal variety of the surrounding sea ice of Zhongshan station. *Chin. J. Polar Res.* **2008**, *20*, 346–354.

25. Cao, J.; Yao, X.J.; Jin, H.A.; Zhang, T.F.; Gao, Y.P.; Zhang, D.H.; Zhao, Q.N. Spatiotemporal variation of ice thickness of Lake Qinghai derived from field measurements and model simulation. *J. Lake Sci.* **2021**, *33*, 607–621.
26. Zhang, X.; Wang, K.; Kirillin, G. An automatic method to detect lake ice phenology using MODIS daily temperature imagery. *Remote Sens.* **2021**, *13*, 2711. [[CrossRef](#)]
27. Cai, Y.; Ke, C.Q.; Li, X.G.; Zhang, G.Q.; Zheng, D.; Lee, H. Variations of lake ice phenology on the Tibetan Plateau from 2001 to 2017 based on MODIS data. *J. Geophys. Res. Atmos.* **2019**, *124*, 825–843. [[CrossRef](#)]
28. Key, J.R.; Mahoney, R.; Liu, Y.H.; Romanov, P.; Tschudi, M.; Appel, I.; Maslanik, J.; Baldwin, D.; Wang, X.J.; Meade, P. Snow and ice products from Suomi NPP VIIRS. *J. Geophys. Res. Atmos.* **2013**, *118*, 816–830. [[CrossRef](#)]
29. Qi, M.M.; Yao, X.J.; Liu, S.Y.; Zhu, Y.; Gao, Y.P.; Liu, B.K. Dynamic change of Lake Qinghai shoreline from 1973 to 2018. *J. Lake Sci.* **2020**, *32*, 573–586.
30. Qi, M.M.; Yao, X.J.; Li, X.F.; An, L.N.; Gong, P.; Gao, Y.P.; Liu, J. Spatial-temporal characteristics of ice phenology of Lake Qinghai from 2000 to 2016. *J. Geogr. Sci.* **2018**, *73*, 932–944.
31. Qi, M.M.; Yao, X.J.; Li, X.F.; Gao, Y.P. A dataset of lake ice phenology in Qinghai Lake from 2000 to 2018. *China Sci. Data* **2018**, *3*, 17–27.
32. Li, X.D.; Zhao, H.F.; Wang, G.X.; Yao, K.R.; Xin, R.; He, Z.L.; Li, L. Influence of watershed hydrothermal conditions and vegetation status on lake level of Qinghai Lake. *Arid Land Geogr.* **2019**, *42*, 499–508.
33. Ke, C.Q.; Xie, H.J.; Lei, R.B.; Li, Q.; Sun, B. Spectral features analysis of sea ice in the Arctic Ocean. *Spectrosc. Spectr. Anal.* **2012**, *32*, 1081–1084.
34. Riggs, G.A.; Hall, D.K.; Salomonson, V.V. A snow index for the Landsat Thematic Mapper and Moderate Resolution Imaging Spectroradiometer. In Proceedings of the IGARSS 1994-1994 IEEE International Geoscience and Remote Sensing Symposium, Pasadena, CA, USA, 8–12 August 1994; pp. 1942–1944.
35. Hall, D.K.; Riggs, G.A.; Salomonson, V.V. Development of methods for mapping global snow cover using Moderate Resolution Imaging Spectroradiometer Data. *Remote Sens. Environ.* **1995**, *54*, 127–140. [[CrossRef](#)]
36. Salomonson, V.V.; Appel, I. Development of the Aqua MODIS NDSI fractional snow cover algorithm and validation results. *IEEE Trans. Geosci. Remote Sens.* **2006**, *44*, 1747–1756. [[CrossRef](#)]
37. Li, X.F. The Development and Application of the Monitoring Method of Lake Ice Based on MODIS Images, A Case of the Qinghai-Tibet Plateau. Master's Thesis, Northwest Normal University, Lanzhou, China, 2018.
38. Kropáček, J.; Maussion, F.; Chen, F.; Hoerz, S.; Hochschild, V. Analysis of ice phenology of lakes on the Tibetan Plateau from MODIS data. *Cryosphere* **2013**, *7*, 287–301. [[CrossRef](#)]
39. O'Reilly, C.M.; Sharma, S.; Gray, D.K.; Hampton, S.E.; Read, J.S.; Rowley, R.J.; Schneider, P.; Lenters, J.D.; McIntyre, P.B.; Kraemer, B.M.; et al. Rapid and highly variable warming of lake surface waters around the globe. *Geophys. Res. Lett.* **2015**, *42*, 10773–10781. [[CrossRef](#)]
40. Noori, R.; Bateni, S.M.; Saari, M.; Almazroui, M.; Haghighi, T. Strong warming rates in the surface and bottom layers of a boreal lake: Results from approximately six decades of measurements (1964–2020). *Earth Space Sci.* **2022**, *9*, e2021EA001973. [[CrossRef](#)]
41. Sharma, S.; Blagrove, K.; Magnuson, J.J.; O'Reilly, C.M.; Oliver, S.; Batt, R.D.; Magee, M.R.; Straile, D.; Weyhenmeyer, G.A.; Winslow, L.; et al. Widespread loss of lake ice around the Northern Hemisphere in a warming world. *Nat. Clim. Chang.* **2019**, *9*, 227–231. [[CrossRef](#)]
42. Li, X.D.; Long, D.; Huang, Q.; Zhao, F.Y. The state and fate of lake ice thickness in the Northern Hemisphere. *Sci. Bull.* **2022**, *67*, 537–546. [[CrossRef](#)]
43. Magnuson, J.J.; Lathrop, R.C. Lake ice: Winter, beauty, value, changes, and a threatened future. *LakeLine* **2014**, *43*, 18–27.
44. Cai, Y.; Ke, C.Q.; Xiao, Y.; Wu, J. What caused the spatial heterogeneity of lake ice phenology changes on the Tibetan Plateau? *Sci. Total Environ.* **2022**, *836*, 155517. [[CrossRef](#)]
45. Caldwell, T.J.; Chandra, S.; Albright, T.P.; Harpold, A.A.; Dilts, T.E.; Greenberg, J.A.; Sadro, S.; Dettinger, M.D. Drivers and projections of ice phenology in mountain lakes in the western United States. *Limnol. Oceanogr.* **2021**, *66*, 995–1008. [[CrossRef](#)]
46. Solarski, M.; Rzetala, M. Determinants of spatial variability of ice thickness in lakes in high mountains of the temperate zone—The case of the Tatra Mountains. *Water* **2022**, *14*, 2360. [[CrossRef](#)]
47. Solarski, M.; Rzetala, M. Changes in the thickness of ice cover on water bodies subject to human pressure (Silesian Upland, Southern Poland). *Front. Earth Sci.* **2021**, *9*, 675216. [[CrossRef](#)]
48. Terzhevik, A.Y.; Pal'shin, N.I.; Golosov, S.D.; Zdorovenov, R.E.; Zdorovenova, G.E.; Mitrokhov, A.V.; Potakhin, M.S.; Shipunova, E.A.; Zverev, I.S. Hydrophysical aspects of oxygen regime formation in a shallow ice-covered lake. *Water Resour.* **2010**, *37*, 568–579. [[CrossRef](#)]
49. Granados, I.; Toro, M.; Giral, S.; Camacho, A.; Montes, C. Water column changes under ice during different winters in a mid-latitude Mediterranean high mountain lake. *Aquat. Sci.* **2020**, *82*, 30. [[CrossRef](#)]
50. Bengtsson, L. Ice-covered lakes: Environment and climate—Required research. *Hydrol. Process* **2011**, *25*, 2767–2769. [[CrossRef](#)]
51. Ke, C.Q.; Cai, Y.; Xiao, Y. Monitoring ice phenology variations in Khanka Lake based on passive remote sensing data from 1979 to 2019. *Natl. Remote Sens. Bull.* **2022**, *26*, 201–210.